Inorganica Chimica Acta, *169* (1990) 109–118

Copper(I) Complexes with Metal–Metal (d^{10}–d^{10}) Bond. Crystal and Molecular Structures of Adducts of Tantalocene Trihydride with Copper(I) Iodide of Composition: $(\eta^5\text{-}C_5H_5)_2TaH[(\mu_2\text{-}H)Cu(\mu_2\text{-}I)_2Cu(\mu_2\text{-}H)]_2HTa(\eta^5\text{-}C_5H_5)_2$, $(\eta^5\text{-}C_5H_4Bu^t)_2TaH(\mu_2\text{-}H)_2Cu(\mu_2\text{-}I)_2Cu(\mu_2\text{-}H)_2HTa(\eta^5\text{-}C_5H_4Bu^t)_2\cdot CH_3CN$ and $\{Cu(\mu_3\text{-}I)\cdot P[N(CH_3)_2]_3\}_4$

T. M. ARKHIREEVA, B. M. BULYCHEV*, A. I. SIZOV, T. A. SOKOLOVA
M. V. Lomonosov Moscow State University, Department of Chemistry, 119899 Moscow (U.S.S.R.)
V. K. BELSKY
L. Ya. Karpov Physico-Chemical Institute, 107120 Moscow (U.S.S.R.)
and G. L. SOLOVEICHIK*
Institute of Chemical Physics, U.S.S.R. Academy of Sciences, 142432 Chernogolovka (U.S.S.R.)

(Received December 10, 1987; revised September 18, 1989)

Abstract

An interaction of copper(I) halogenides with tantalocene trihydride Cp'_2TaH_3 led to adducts of 2:1 ($Cp = \eta^5\text{-}C_5H_5$) or 1:1 ($Cp' = C_5H_5Bu^t$) composition. Structures of complexes $(\eta^5\text{-}C_5H_5)_2\text{-}TaH[(\mu_2\text{-}H)Cu(\mu_2\text{-}I)_2Cu(\mu_2\text{-}H)]_2TaH(\eta^5\text{-}C_5H_5)$ (I) and $(\eta^5\text{-}C_5H_4Bu^t)_2TaH(\mu_2\text{-}H)_2Cu(\mu_2\text{-}I)Cu(\mu_2\text{-}H)_2\text{-}TaH(\eta^5\text{-}C_5H_4Bu^t)_2$ (III) were established by X-ray analysis. Crystals of **I** are monoclinic: $a = 8.010$, $b = 11.032$, $c = 16.613$ Å, $\gamma = 105.1°$, space group $I2/m$, $Z = 2$, $R = 0.20$. Crystals of **III** are monoclinic: $a = 16.378(4)$, $b = 16.968(4)$, $c = 16.607(4)$ Å, $\gamma = 113.57(3)°$, space group $P2_1/b$, $Z = 4$, $R = 0.031$ ($R_w = 0.031$). In both complexes the $Cu(\mu_2\text{-}I)_2Cu$ moiety is bonded with tantalum atoms by one (**I**, Ta .... Cu = 2.788 Å) or two (**III**, Cu....Cu = 2.844 Å) hydrogen bridges.

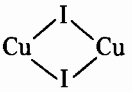

rhombs are not planar owing to the formation of the direct intermetal bonds between Cu(I) atoms (Cu....Cu distance is equal to 2.602 Å for **I** and 2.913 Å for **III**). The model of bonding in $L_nCu(\mu_2\text{-}I)_2CuL_n$ complexes has been proposed and the conditions of realization of the bond between transition metal atoms with a d^{10} electron shell are discussed.

It is shown that the conditions of $n = 2$ and bulky ligand L are essential but insufficient, e.g. the 1:1 adduct of Cu(I) with bulky phosphine $P(NMe_2)_3$ is a tetramer $[Cu(\mu_3\text{-}I)\cdot P(NMe_2)_3]_4$ (**V**) without Cu–Cu bonds. Crystals of **V** are monoclinic: $a = 14.695(5)$, $b = 14.999(5)$, $c = 23.406(8)$ Å, space group $P2_1/n$, $Z = 4$, $R = 0.039$ ($R_w = 0.040$).

Introduction

According to X-ray structure analysis practically all adducts of copper(I) halogenides with organic Lewis bases are crystallized in the form of dimers or polymers with halogen bridging atoms forming a planar metallocycle $Cu(\mu_2\text{-}X)_2Cu$ [1, 2]. Analogous dimerization also occurs in the CuI complex with the organometallic base Cp_2MoH_2 ($Cp = \eta^5\text{-}C_5H_5$) of composition $Cp_2Mo(\mu_2\text{-}H)_2Cu(\mu_2\text{-}I)_2\text{-}Cu(\mu_2\text{-}H)_2MoCp_2$ (Cu....Cu = 3.33 Å) [3]. However, it was found that a complex based on Cp_2ReH of $[Cp_2ReH\cdot CuI]_2$ composition apart from bridging bonds $Cu(\mu_2\text{-}I)_2Cu$ between copper(I) atoms with electronic configuration d^{10} realizes in its structure a unique Cu–Cu bond with length 2.55 Å [4]. A short bond length Cu–Cu = 2.72 Å has been noted previously in the T-frame cluster $[Cp_2MoH_2]_2\text{-}Cu[CuCl_2]$ [5]. A shorter interatomic Cu–Cu distance in this compound, however, is more likely to be attributed to the binding metal–hydride interaction in the moiety

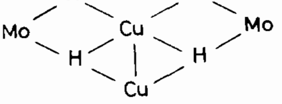

Cp_2ReH and Cp_2MoH_2 are d^4 and d^2 bases respectively and, thus, have two centers of basicity: nucleophilic hydride atoms and lone d-electron pairs. Since the contribution of the latter in the Cu–Cu

---

*Authors to whom correspondence should be addressed.

0020-1693/90/$3.50

bond formation in complexes $(Cp_2MH_n\cdot CuX)_2$ (M = Mo, W, Re) and their effect on the compound structures is still not clear [3–5], we have synthesized and studied by the single-crystal X-ray technique the copper-bearing adducts of tantalocene trihydride (Cp_2TaH_3) with no lone d-electron pairs (d^0-base) which, consequently, can bind with CuX (and with other Lewis acids) solely via hydrogen bridging atoms.

Experimental

The synthesis and preparation of samples for physical and chemical analyses were performed under vacuum or in dry argon.

Acetonitrile (AN) was refluxed over CaH_2 for 1.5–2 h with further distillation.

Tantalocene trihydride was prepared by a modified literature procedure [6]. Substituted tantalocene trihydride, $(C_5H_4Bu^t)_2TaH_3$, was synthesized analogously by using tert-butylcyclopentadiene prepared by the procedure from ref. 7.

Anhydrous copper(I) iodide of 'chemically pure' grade was used without additional purification.

Anhydrous copper(I) chloride was obtained via $CuCl_2$ reduction by boiling in glycerin [8].

The IR spectra of the samples (suspension in Nujol) were recorded in the region 400–3500 cm^{-1} on a UR-20 spectrophotometer.

Metal content of the synthesized compounds was determined by X-ray fluorescence analysis on a VRA-20 Instrument (W anode, 15 kV, 10 A; crystal analyser LiF-200, exposure 10 and 100 s, analytical lines for Ta: $L_{\alpha 1} = 44.4$ and $L_{\beta 1} = 38.47$, analytical lines for Cu: $K_{\alpha 1} = 44.96$, $K_{\beta 1} = 40.44$.

Cp_2TaH_3 complexes with copper(I) halogenides were prepared by the standard procedure. To a solution of 0.3 g (1 mmol) Cp_2TaH_3 in 30 ml of AN, 20 ml of 0.1 mmol CuX solution were added dropwise in the same solvent. The mixture was stirred for 30 min. The precipitate was filtered off, washed on a filter with 2 × 5 ml of AN and dried under vacuum.

White fine crystalline substances of composition $Cp_2TaH_3\cdot 2CuI$ (I), $Cp_2TaH_3\cdot 2CuCl$ (II), $(C_5H_4Bu^t)_2TaH_3\cdot CuI\cdot 0.5CH_3CN$ (III) and $CuI\cdot CH_3CN$ (IV) were obtained.

$Cp_2TaH_3\cdot 2CuI$ (I). Anal. Found: Ta, 26.0; Cu, 18.0; C, 17.4; H, 2.1; I, 36.6. Calc. for $C_{10}H_{13}TaCu_2I_2$: Ta, 26.0; Cu, 18.3; C, 17.3; H, 1.9; I, 36.5%.

$Cp_2TaH_3\cdot 2CuCl$ (II). Anal. Found: Ta, 33.3; Cu, 27.7; C, 22.3; H, 2.7; Cl, 14.0. Calc. for $C_{10}H_{13}TaCu_2Cl_2$: Ta, 35.3; Cu, 24.8; C, 23.4; H, 2.6; Cl, 13.9%.

$(C_5H_4Bu^t)_2TaH_3\cdot CuI\cdot 0.5CH_3CN$ (III). Anal. Found: Ta, 27.7; Cu, 9.2; C, 37.5; H, 2.9; I, 20.4. Calc. for $C_{18}H_{26}TaCuI\cdot 0.5CH_3CN$: Ta, 28.41; Cu, 9.9; C, 37.7; H, 2.98; I, 19.9%.

At excess CuI super stoichiometry of complexes I and III, a mixture of substances is crystallized from the solution: colorless crystals of complexes I and III and light yellow crystals $CuI\cdot CH_3CN$ (IV).

$CuI\cdot CH_3CN$ (IV). Anal. Found: Cu, 27.7; I, 54.2. Calc. for $CuICH_3CN$: Cu, 27.3; I, 54.98%.

Single crystals of complexes I and III were isolated under slow evaporation of the filtrate after its separation from the major bulk of crystals of the corresponding complexes.

$CuI\cdot P[N(CH_3)_2]_3$ (V) was obtained by interaction of 2.8 g CuI in 100 ml AN with an equimolar amount of $P[N(CH_3)_2]_3$. The solution was evaporated to half of the starting volume and cooled to

TABLE 1. Crystal data for the complexes $(Cp_2TaH_3\cdot 2CuI)_2$ (I), $(C_5H_4Bu^t)_2TaH_3\cdot CuI_2\cdot CH_3CN$ (III), $(CuI\cdot CH_3CN)_x$ (IV) and $[CuI\cdot P(NMe_2)_3]_4$ (V)

	I	III	IV	V
Formula	$C_{20}H_{26}Ta_2Cu_4I_4$	$C_{38}H_{61}NTa_2Cu_2I_2$	C_2H_3NCuI	$C_{24}H_{72}N_{12}P_4Cu_4I_4$
Lattice	monoclinic	monoclinic	rhombic	monoclinic
Space group	*I2/m*	$P2_1/b$	*Pmnb*	$P2_1/n$
a (Å)	8.010	16.378(4)	4.239(1)	14.694(5)
b (Å)	11.032	16.968(4)	8.778(1)	14.999(5)
c (Å)	16.631	16.507(4)	13.628(2)	23.406(8)
γ (°)	105.10	113.57(3)	90	93.16(3)
V (Å^3)	1417.3	4204.6	513.0	5150(3)
Z	2	4	4	4
D_{calc} (g/cm^3)	1.63	1.33	3.00	1.82
μ(Mo Kα) (cm^{-1})		79.4	100.5	42.7
No. reflections with $I \geqslant 3\sigma(I)$	1230	2472	466	3181
R	0.20[a]	0.031	0.026	0.039
R_w		0.031		0.040

[a] Unfortunately, it has not been possible to refine the structure due to a poor quality of the single crystal used.

+5 °C. Crystals precipitated after 12 h, were separated from the mother liquor, washed with ether and dried under vacuum. *Anal.* Found: Cu, 17.3; I, 35.4. Calc. for $CuIPN_3C_6H_{18}$: Cu, 17.96; I, 35.93%.

The X-ray diffraction analysis of **I**, **III**, **IV** and **V** was performed on a Syntex P$\bar{1}$ diffractometer (Mo Kα radiation, graphite monochromator, $\theta/2\theta$ scanning) (Table 1).

TABLE 2. Atomic coordinates and thermal parameters for the complex $(C_5H_4Bu^t)_2TaH(\mu_2\text{-}H)_2Cu(\mu_2\text{-}I)_2Cu(\mu_2\text{-}H)_2HTa(C_5H_4Bu^t)_2$

Atom	x	y	z	U_{eq}
Ta(1)	0.0772(1)	0.2998(1)	0.3847(1)	0.041(1)
Ta(2)	0.4596(1)	0.3059(1)	0.0365(1)	0.037(1)
I(1)	0.3764(1)	0.3404(1)	0.3084(1)	0.058(1)
I(2)	0.2227(1)	0.3911(1)	0.1221(1)	0.083(1)
Cu(1)	0.2183(2)	0.3377(1)	0.2709(1)	0.058(1)
Cu(2)	0.3513(2)	0.3329(1)	0.1515(1)	0.053(1)
C(1)	0.1248(11)	0.2532(9)	0.5078(8)	0.035(7)
C(2)	0.6120(12)	0.2889(11)	0.5262(10)	0.054(9)
C(3)	0.1022(14)	0.3752(11)	0.5059(10)	0.073(10)
C(4)	0.1848(11)	0.3956(10)	0.4753(10)	0.061(9)
C(5)	0.1957(11)	0.3198(12)	0.4745(9)	0.045(8)
C(6)	0.1210(11)	0.1653(10)	0.5368(10)	0.050(8)
C(7)	0.0292(11)	0.1030(11)	0.5577(11)	0.069(9)
C(8)	0.1782(12)	0.1806(10)	0.6136(10)	0.058(9)
C(9)	0.1576(11)	0.1254(11)	0.4704(10)	0.063(9)
C(11)	−0.0650(11)	0.2193(10)	0.3205(10)	0.044(9)
C(12)	−0.0088(11)	0.2770(9)	0.2640(9)	0.049(8)
C(13)	0.0115(12)	0.3617(11)	0.2889(12)	0.077(9)
C(14)	−0.0263(12)	0.3629(9)	0.3634(12)	0.071(10)
C(15)	−0.0765(11)	0.2700(12)	0.3837(12)	0.069(9)
C(16)	−0.1190(11)	0.1247(10)	0.3054(9)	0.043(8)
C(17)	−0.1987(13)	0.1130(11)	0.2501(12)	0.089(11)
C(18)	−0.0676(14)	0.0837(13)	0.2629(12)	0.087(11)
C(19)	−0.1572(12)	0.0768(10)	0.3830(11)	0.069(8)
C(21)	0.5344(12)	0.2283(10)	0.1086(10)	0.048(9)
C(22)	0.5341(11)	0.2958(11)	0.1607(9)	0.043(8)
C(23)	0.5865(11)	0.3764(10)	0.1213(12)	0.075(9)
C(24)	0.6171(12)	0.3586(14)	0.0479(13)	0.067(10)
C(25)	0.5816(11)	0.2666(11)	0.0405(11)	0.052(9)
C(26)	0.5064(13)	0.1360(11)	0.1316(11)	0.055(9)
C(27)	0.4218(13)	0.1086(11)	0.1816(11)	0.089(11)
C(28)	0.5789(12)	0.1281(12)	0.1877(12)	0.073(9)
C(29)	0.5006(19)	0.0799(12)	0.0589(12)	0.109(15)
C(31)	0.3745(10)	0.2500(10)	−0.0862(8)	0.034(8)
C(32)	0.4665(14)	0.2922(12)	−0.1047(10)	0.068(10)
C(33)	0.4928(13)	0.3810(12)	−0.0891(11)	0.063(10)
C(34)	0.4214(16)	0.3945(12)	−0.0574(12)	0.071(11)
C(35)	0.0487(12)	0.3108(11)	−0.0529(9)	0.048(8)
C(36)	0.3099(11)	0.1590(10)	−0.2104(10)	0.046(8)
C(37)	0.2687(11)	0.1696(9)	−0.1891(9)	0.058(8)
C(38)	0.2343(12)	0.1187(11)	−0.0495(11)	0.063(9)
C(39)	0.3616(13)	0.1036(10)	−0.1246(11)	0.073(9)
N	0.0731(16)	0.0818(18)	0.0961(14)	0.140(17)
C(40)	0.1285(18)	0.0940(17)	0.1485(18)	0.103(15)
C(41)	0.1885(14)	0.1032(14)	0.2140(14)	0.105(12)
H(1)	0.144(6)	0.373(5)	0.328(5)	
H(2)	0.128(6)	0.249(5)	0.324(5)	
H(3)	0.039(6)	0.217(5)	0.382(5)	
H(4)	0.447(6)	0.369(5)	0.079(5)	
H(5)	0.388(6)	0.267(5)	0.891(5)	
H(6)	0.409(6)	0.229(5)	0.029(5)	

Atom coordinates in complexes **III**, **IV** and **V** are listed in Tables 2–4, and main interatomic distances and valency angles are given in Tables 5–8.

TABLE 3. Atomic coordinates and thermal parameters for the complex $[\mathrm{CuI \cdot CH_3CN}]_x$

Atom	x	y	z	U_{eq}
I	0.7500	0.5313(1)	0.6378(1)	0.0497(4)
Cu	0.7500	0.5914(3)	0.4480(2)	0.0633(9)
N	0.7500	0.8132(19)	0.4204(12)	0.061(6)
C(1)	0.7500	0.9361(20)	0.3978(12)	0.043(6)
C(2)	0.7500	1.0938(26)	0.3691(13)	0.065(7)
H(1)	0.7500	1.092	0.319	
H(2)	0.891	1.155	0.399	

TABLE 4. Atomic coordinates and thermal parameters for the complex $\{\mathrm{CuI \cdot P[N(CH_3)_2]_3}\}_4$

Atom	x	y	z	U_{eq}
I(1)	0.2838(1)	0.3649(1)	0.0392(1)	0.063(1)
I(2)	0.1321(1)	0.2586(1)	0.1825(1)	0.074(1)
I(3)	0.2868(1)	0.0938(1)	0.0750(1)	0.066(1)
I(4)	0.4161(1)	0.2735(1)	0.1903(1)	0.069(1)
Cu(1)	0.2758(2)	0.3729(1)	0.1550(1)	0.80(1)
Cu(2)	0.1677(1)	0.2264(1)	0.0716(1)	0.074(1)
Cu(3)	0.4037(1)	0.2426(1)	0.0764(1)	0.081(1)
Cu(4)	0.2743(1)	0.1493(1)	0.1863(1)	0.088(1)
P(1)	0.2754(3)	0.5056(3)	0.1978(2)	0.075(2)
P(2)	0.0415(4)	0.2145(3)	0.0185(2)	0.086(2)
P(3)	0.5361(3)	0.2336(2)	0.0309(1)	0.071(2)
P(4)	0.2698(3)	0.0421(2)	0.2527(2)	0.074(2)
N(11)	0.1940(11)	0.5705(10)	0.1766(7)	0.123(8)
N(12)	0.2603(10)	0.5052(10)	0.2700(6)	0.103(7)
N(13)	0.3739(10)	0.5646(9)	0.1931(7)	0.114(7)
N(21)	−0.0314(8)	0.1296(9)	0.0397(7)	0.104(7)
N(22)	0.0638(11)	0.2091(10)	−0.0516(7)	0.115(8)
N(23)	−0.0291(12)	0.3038(12)	0.0214(9)	0.160(10)
N(31)	0.6148(9)	0.1662(8)	0.0598(6)	0.076(6)
N(32)	0.5987(8)	0.3298(8)	0.0287(6)	0.087(6)
N(33)	0.5257(9)	0.1882(9)	−0.0335(6)	0.086(6)
N(41)	0.3591(10)	−0.0226(11)	0.2569(7)	0.120(8)
N(42)	0.1852(9)	−0.0335(9)	0.2460(6)	0.103(6)
N(43)	0.2681(13)	0.0804(11)	0.3199(6)	0.137(9)
C(111)	0.1456(12)	0.5545(13)	0.1246(8)	0.120(9)
C(112)	0.1774(18)	0.6559(14)	0.2005(11)	0.232(15)
C(121)	0.1737(17)	0.4689(16)	0.2893(9)	0.168(13)
C(122)	0.3316(19)	0.4651(17)	0.3007(9)	0.182(14)
C(131)	0.4370(14)	0.5501(15)	0.1472(10)	0.154(11)
C(132)	0.4036(18)	0.6430(15)	0.2268(11)	0.195(14)
C(211)	−0.0048(12)	0.0615(12)	0.0778(8)	0.129(9)
C(212)	−0.1239(13)	0.1184(14)	0.0167(11)	0.151(11)
C(221)	0.1475(16)	0.1746(13)	−0.0695(7)	0.140(10)
C(222)	−0.0037(18)	0.2076(17)	−0.0962(10)	0.191(15)
C(231)	0.0099(19)	0.3830(12)	−0.0053(14)	0.270(18)
C(232)	−0.0662(16)	0.3159(19)	0.0786(12)	0.224(15)
C(311)	0.5879(12)	0.0707(10)	0.0589(8)	0.108(8)
C(312)	0.6526(11)	0.1930(13)	0.1152(7)	0.105(8)
C(321)	0.6897(11)	0.3375(12)	0.0031(10)	0.133(10)
C(322)	0.5587(12)	0.4121(10)	0.0355(9)	0.110(8)
C(331)	0.4457(12)	0.1981(12)	−0.0647(8)	0.111(9)

(continued)

TABLE 4. *(continued)*

Atom	*x*	*y*	*z*	U_{eq}
C(332)	0.6010(14)	0.1609(14)	−0.0661(8)	0.139(10)
C(411)	0.3998(21)	−0.0504(21)	0.2120(11)	0.257(18)
C(412)	0.4234(26)	0.0312(31)	0.2855(23)	0.571(37)
C(421)	0.1240(15)	−0.0339(14)	0.2047(10)	0.201(13)
C(431)	0.2139(16)	0.1527(20)	0.3333(8)	0.192(14)
C(422)	0.1711(19)	−0.1069(16)	0.2868(14)	0.288(19)
C(432)	0.2582(31)	0.0362(28)	0.3675(17)	0.411(40)

TABLE 5. Main interatomic distances and bond angles in the complex $[Cp_2TaH_3 \cdot 2CuI]_2$

Bond	*d* (Å)	Angle	ω (°)
Ta–C(1)	2.35	TaCuCu′	143.1
Ta–C(2)	2.39	CuTaCu′*	73.9
Ta–C(3)	2.39	I(1)CuI(2)	107.8
Ta–C(4)	2.35	CuI(1)Cu′	58.7
Ta–C(5)	2.32	CuI(2)Cu′	59.2
Ta··Cu	2.788	Cu′CuI(1)	60.6
Cu–Cu′	2.602	Cu′CuI(2)	60.4
Cu–I(1)	2.653	CuCu′I(1)/CuCu′I(2)	136.3
Cu–I(2)	2.635	I(1)CuI(2)/I(1)Cu′I(2)	122.1
I(1)··I(2)	4.273		
Cu··Cu′*	3.352		

Cu′* is atom of neighbouring rhombus Cu_2I_2 connected to Cu′ by inversion operation.

TABLE 6. Main interatomic distances in the complex $[(C_5H_4Bu^t)_2Ta(H)(\mu_2\text{-}H)_2Cu(\mu_2\text{-}I)]_2$

Bond	*d* (Å)	Bond	*d* (Å)
Ta1–C1	2.42(2)	Ta2–C33	2.38(2)
Ta1–C2	2.35(2)	Ta2–C34	2.41(2)
Ta1–C3	2.32(2)	Ta2–C35	2.41(2)
Ta1–C4	2.39(2)	C31–C36	1.54(2)
Ta1–C5	2.36(2)	Ta2–C (av.)	2.39
Ta1–C11	2.42(2)	$(C-C)^{Cp}$ (av.)	1.41
Ta1–C12	2.38(2)	$(C-C)^{Bu}$ (av.)	1.52
Ta1–C13	2.38(2)	Ta1–H1	1.59(8)
Ta1–C14	2.37(2)	Ta1–H2	1.73(10)
Ta1–C15	2.36(2)	Ta1–H3	1.29(8)
C1–C6	1.55(3)	H1–Cu1	1.81(9)
C11–C16	1.51(2)	H2–Cu1	1.85(8)
Ta1–C (av.)	2.37	Ta1··Cu1	2.844(2)
$(C-C)^{Cp}$ (av.)	1.41	Cu1–I1	2.630(3)
$(C-C)^{Bu}$ (av.)	1.51	Cu1–I2	2.608(3)
Ta2–C21	2.44(2)	Cu1–Cu2	2.913(3)
Ta2–C22	2.43(2)	Cu2–I1	2.622(3)
Ta2–C23	2.39(2)	Cu2–I2	2.593(3)
Ta2–C24	2.38(2)	Cu2··Ta2	2.836(3)
Ta2–C25	2.35(2)	Cu2–H4	1.87(10)
C21–C26	1.43(2)	Cu2–H5	1.91(9)
Ta2–C31	2.43(2)	Ta2–H4	1.37(10)
Ta2–C32	2.35(2)	Ta2–H5	1.43(9)
		Ta2–H6	1.24(8)

TABLE 7. Bond angles in the complex $[(C_5H_4Bu^t)_2Ta(H)(\mu_2\text{-}H)_2Cu(\mu_2\text{-}I)]_2$

Angle	ω (°)	Angle	ω (°)
CpI/CpII	43.6	Ta1Cu1Cu2	169.6
CpITa1CpII	139.6	Ta2Cu2Cu1	166.7
CpIII/CpIV	43.2	I1Cu1I2	108.9(1)
CpIIITa2CpIV	139.7	I1Cu2I2	109.7(1)
H1Ta1H2	74.0(4.5)	Cu1I1Cu2	67.4(1)
H2Ta1H3	64.4(4.8)	Cu1I2Cu2	68.1(1)
H1Ta1H3	135.7(5.1)	H1Cu1H2/H1Ta1H2	169.9
H1Cu1H2	66.8	Cu1I1Cu2/Cu1I2Cu2	158.5
H4Ta2H5	71.6(5.0)	I1Cu1I2/I1Cu2I2	148.9
H5Ta2H6	59.5(5.6)	CpI/C1–C6	12.1
H4Ta2H6	129.3(5.5)	CpII/C11–C16	12.4
H4Cu2H5	51.2		

Results and Discussion

Interaction of Cp_2TaH_3 with copper(I) halogenides yields the complexes of composition $Cp_2TaH_3 \cdot 2CuX$, the stoichiometry of which differs from that in the previously synthesized complexes based on Cp_2MoH_2 [3] and Cp_2ReH [4]. The IR spectra of **I** and **II** revealed absorption bands, assigned to valency and deformation vibration of terminal and bridging bonds Ta–H: $\nu(Ta–H^t) = 1790$ and 1810 cm^{-1}, $\nu(Ta–H^b) = 1515$ and 1580 cm^{-1}, $\delta(H^tTaH^b) = 780$ cm^{-1}, $\delta(TaH_2{}^b) = 730$, 740 and 735, 745 cm^{-1} respectively. It is noteworthy that slight oxidation of the samples by the air decreases primarily the intensity of the absorption bands of Ta–H (1790–1810 and 780 cm^{-1}) terminal bonds vibrations. The IR spectroscopy analysis has confirmed that Ta and Cu atoms in complexes **I** and **II** are bound by single-bridge Ta–H–Cu bonds. Unfortunately, the poor quality of the single crystals of **I** and high molecular symmetry prevented a comprehensive structural experiment for this substance and hydrogen atoms localization from being carried out. However, the position of the heavy atoms (continuous line in Fig. 1) was determined reliable enough. Figure 1 shows dimer molecule **I** with two metal cycles $Cu(\mu_2\text{-}I)_2Cu$ with

TABLE 8. Main interatomic distances and bond angles in the complexes $[CuI{\cdot}P(NMe_2)_3]_4$ and $[CuI{\cdot}CH_3CN]_x$

$[CuI{\cdot}P(NMe_2)_3]_4$				$[CuI{\cdot}CH_3CN]_x$			
Bond	d (Å)	Angle	ω (°)	Bond	d (Å)	Angle	ω (°)
Cu–I (av.)	2.73(2)	CuICu (av.)	76.8(1.5)	Cu–I (av.)	2.66(1)	CuICu	69.6(1)
Cu–P (av.)	2.23(1)	ICuI (av.)	101.8(2.0)	Cu–N	1.98(2)	Cu(1)ICu(2)	106.9(1)
P–N (av.)	1.68(3)			N–C	1.22(2)	ICuI	110.4(1)
N–C (av.)	1.42(5)			C–C	1.44(3)	I(1)CuI(2)	106.9(1)
Cu··Cu	3.385			Cu··Cu	3.331		
I··I	4.23						

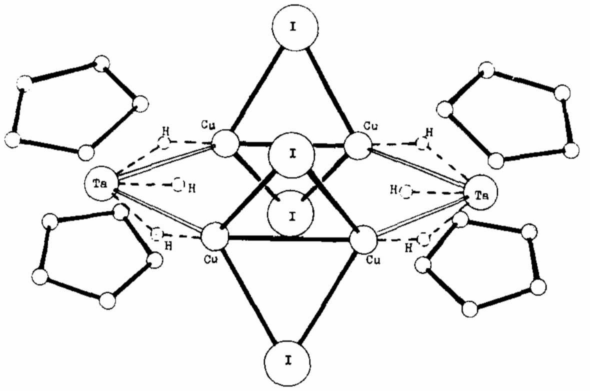

Fig. 1. The structure of the complex $(\eta^5\text{-}C_5H_5)TaH[(\mu_2\text{-}H)\text{-}Cu(\mu_2\text{-}I)Cu(\mu_2\text{-}H)]_2HTa(\eta^5\text{-}C_5H_5)_2$ (dotted lines denote the supposed position of the hydrogen atoms).

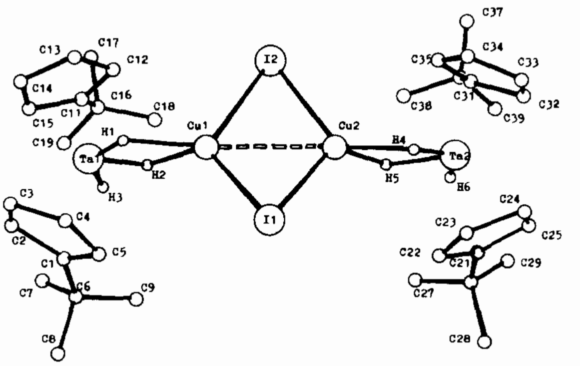

Fig. 2. The structure of the complex $(C_5H_4Bu^t)_2TaH(\mu\text{-}H)_2\text{-}Cu(\mu_2\text{-}I)_2Cu(\mu_2\text{-}H)_2HTa(C_5H_4Bu^t)_2$.

parameters close to that found in $[Cp_2ReH{\cdot}CuI]_2$ [4] (Table 9). These moieties are rhombii with parallel equal sides bent along the I–I axis caused by the Cu–Cu (2.60 Å) bond formation. Copper atoms of different metal cycles do not have binding contacts (3.35 Å). Though the Ta....Cu distances in **I** (Table 9) are less than the sum of the covalent radii in the tantalum and copper atoms (1.57 [9] + 1.38 [10] Å), the IR spectra, stoichiometry of complexes and its diamagnetism point to the absence of a direct Ta–Cu bond. Attempts to grow a more perfect single crystal of complex **I** were unsuccessful. Thus, we have synthesized analogue **I** with tert-butyl substitutes in the cyclopentadienyl rings.

$(C_5H_4Bu^t)_2TaH_3$ also forms a copper(I) iodide adduct. However, the introduction of bulky tert-C_4H_9 groups led to changes of the compound composition. Unlike Cp_2TaH_3 which yields a CuI complex with ratio Ta:Cu = 1:2, a complex of $[(C_5H_4\text{-}Bu^t)_2TaH_3{\cdot}CuI]_2{\cdot}CH_3CN$ composition (**III**) is crystallized from acetonitrile solution with $(C_5H_4Bu^t)_2\text{-}TaH_3$ and CuI with ratio Ta:Cu 1:1, and with ratio Ta:Cu 1:2 a complex of composition **III** and $(CuI{\cdot}CH_3CN)_x$ (**IV**).

The present paper does not discuss $(CuICH_3CN)_x$ as this compound structure is quite ordinary for this type of complex and correlates well with that previously published [2].

The X-ray diffraction analysis of **III** has shown that the complex is formed out of dimer molecules $(C_5H_4Bu^t)_2TaH(\mu_2\text{-}H)_2Cu(\mu_2\text{-}I)_2Cu(\mu_2\text{-}H)_2HTa(C_5\text{-}H_4Bu^t)_2$ (Fig. 2) and crystal acetonitrile molecules separated by simple van der Waals contacts. Cyclopentadienyl rings are found on eclipsed conformation, and tert-butyl groups of both $(C_5H_4Bu^t)_2Ta$ moieties are oriented in one direction (Fig. 2). This seems to be the precise reason why the coordination of yet another $Cu(\mu_2\text{-}I)_2Cu$ is prevented, and, consequently, the adduct formation of $(C_5H_4\text{-}Bu^t)_2TaH_32CuI$ composition is prevented as well. Cavities between Bu^t-groups are filled with the AN molecules.

The structure of the $(C_5H_4Bu^t)_2TaH_3$ moieties (Table 6) is similar to the structure of an individual Cp_2TaH_3 [11] molecule and Cp_2TaH_3 moiety in complexes $Cp_2TaH_3{\cdot}ZnCl_2{\cdot}THF$ [12] and $[(C_5H_4\text{-}Bu^t)_2TaH_3{\cdot}ZnCl_2]_2$ [13], with the average Ta–C distance being 2.39, 2.37 and 2.38 Å, and the CpTaCp angle being 140°, 138.9° and 139.8° respectively (2.37, 2.39 Å and 139.6° in complex **III**). The tert-butyl groups go out from the cyclopentadienyl ring planes in the direction of the Ta atoms: the angle between the plane and ring tertiary carbon atom makes approximately 12°. Deviation of the tertiary carbon atoms of the Bu^t groups from the ring plane is 0.32 Å, which is somewhat greater than the relative deviation in complexes $(C_5H_4Bu^t)_2$-$TiCl_2$ and $[(C_5H_4Bu^t)_2TaH_3\cdot ZnCl_2]_2$ with the Bu^t-groups oriented in the opposite directions (0.27 Å [14] and 0.31, 0.26 Å [13] respectively).

The Ta and Cu atoms in **III** are bound by two bridging atoms of hydrogen. A similar binding mode for Ta is realized in complexes $Cp_2TaH_3\cdot ZnCl_2\cdot$ THF [12] and $[(C_5H_4Bu^t)_2TaH_3\cdot ZnCl_2]_2$ [13], and for Cu in complex $(Cp_2MoH_2\cdot CuI)_2$ [3]. In spite of the low accuracy in determination of the hydrogen hydride atom coordinates it is noteworthy that the Ta–H terminal bond length is shorter by 0.2–0.3 Å than that of the bridging one, and the bridge itself is asymmetrical (Table 6). The valency angles H^tTaH^b and H^bTaH^b in **III** within the measurement errors correlate well with those in complex $Cp_2TaH(\mu_2\text{-}H)_2ZnCl_2\cdot$THF (61 and 72°) [12], but greater than in $[(C_5H_4Bu^t)_2$-$TaH_3\cdot ZnCl_2]_2$ (56 and 63°) [13]. The Cu–H bond length in **III** is quite common for complexes with hydrogen bridging atoms (1.6–2.0 Å) [3, 5, 15].

The $Cu(\mu_2\text{-}I)_2Cu$ metal cycle is a central nucleus of complex **III**. The Cu–I bond length in **III** does practically not differ from r(Cu–I) in **I** and in complexes CuI with Cp_2MoH_2 and Cp_2ReH (Table 9). However, the Cu–Cu distance in **III** (2.91 Å) is intermediate between the Cu–Cu bond length in $(Cp_2ReH\cdot CuI)_2$ and in complex **I** on the one hand, and disconnective contact Cu....Cu in complexes $(CuI\cdot CH_3CN)_x$ and $(Cp_2MoH_2\cdot CuI)_2$ (Table 9), on the other hand. Though this distance is greater than the sum of the covalent radii of the copper atoms (1.38 + 1.38 Å), the $Cu(\mu_2\text{-}I)_2Cu$ rhombus bent along the I....I axis (dihedral angle is 148.9°) is indisputable evidence of a direct copper–copper bond in molecule **III**. Therefore, **III** as well as **I** is a diamagnetic compound (definition of μ_{eff} at 77–293 K).

Dissolving $[(C_5H_4Bu^t)_2TaH_3\cdot CuI]_2$ in acetonitrile led to rupture of the $Ta\text{–}H_B\text{–}Cu$ bond, proved by the proton H_B(doublet) and C_5H_4 signals shift in the PMR spectra into the weak field (Table 10) and of the H_A proton signal into the strong field as compared to the spectra position of an individual Cp_2TaH_3 and $(C_5H_4Bu^t)_2TaH_3$. Similar changes in the position of the proton signals in heterometallic complexes based on tantalocene trihydride and Group IIA metal halogenides and their inversion have been described [12]. Thus, unlike the crystal state in solution, the Ta atom in complex **III** is bound to the Cu atom via a single hydrogen bridge Ta–H–Cu. It is still not known whether the dimer structure of the complex with a Cu–Cu bond remains after dissolving or whether a much deeper dissociation with rupture of the Cu–I bonds occurs.

TABLE 9. Structural parameters for the $Cu(\mu_2\text{-}I)Cu$ moiety in copper(I) adducts with transition metal bis(cyclopentadienyl) hydrides

Complex	M–Cu d (Å)	Cu–Cu d (Å)	Cu–I(1) d (Å)	Cu–I(2) d (Å)	MCuCu' ω (°)	CuICu' ω (°)	I(1)CuI(2) ω (°)	$Cu_2I(1)/Cu_2I(2)$ ω (°)	I_2Cu/I_2Cu' ω (°)	References
$[Cp_2ReH\cdot CuI]_2$	2.60	2.55	2.58	2.75	140.5	57.2	103.0	126.1	100.5	4
$[Cp_2TaH_3\cdot 2CuI]_2$	2.79	2.60	2.64	2.65	143.1	58.7 59.2	107.8	136.2	122.1	this work
$[(C_5H_4Bu^t)_2TaH_3\cdot CuI]_2$	2.84	2.91	2.61 2.63	2.59 2.62	169.6 166.7	67.4 68.1	108.9 109.7	158.5	148.9	this work
$[Cp_2MoH_2\cdot CuI]_2$	2.73	3.33	2.60	2.64	180	75.5	104.6	180	180	3
$[CuI\cdot CH_3CN]_x$	–	3.03	2.64	2.67	–	69.6	110.4	180	180	2 and this work

TABLE 10. ^1H NMR spectroscopic parameters for Cp'_2TaH_3 and $[(C_5H_4Bu^t)_2TaH_3 \cdot CuI]_2$

Compound	δ (ppm)				Solvent
	H_A	H_B	Cp	CH_3	
$(C_5H_5)_2TaH_3$	−2.45t −2.40t	−3.40d −3.32d	5.2 5.2		C_6D_6 d_6-DMSO
$(C_5H_4Bu^t)_2TaH_3$	−2.15t	−3.10d	5.02d	1.12s	CD_3CN
$[(C_5H_4Bu^t)_2TaH_3 \cdot CuI]_2$	−2.52d	−3.73t	5.33d	1.00s	CD_3CN

t, triplet; d, doublet; s, singlet.

The most interesting problems in the structure of complexes **I** and **III** are related to the nature of the direct bond between the copper atoms with a d^{10} configuration as well as to the reasons for their occurrence. Until now it was postulated that metal–metal interaction in the case of a filled d-shell is impossible [16] or negligible [17]. However, calculations carried out non-empirically on an extended basis have shown that Cu–Cu bond formation in molecule Cu_2 is considerably contributed to by both s-orbitals and by inner d-orbitals [18]. Previously we have suggested that the Cu–Cu bond formation in the $Cp_2ReHCuI$ complex is realized namely by the binding of d electrons. This fact, in its turn, presupposes the possibility of dsp^3 hybridization of the copper atoms. There are two types of hybrid dsp^3 orbital orientations corresponding to two coordination polyhedrons – trigonal bipyramid and tetragonal pyramid. The copper-bearing complexes based on rheniocene hydride and tantalocene trihydride realize the latter case. Here in the simplest case, out of four hybrid orbitals directed to the pyramid base two are used to form covalent and donor–acceptor bonds with iodide atoms and the two latter to form two bent Cu–Cu bonds. An axial vacant orbital is used to form a donor–acceptor bond with an organometallic molecule moiety. The qualitative scheme of MO moieties LCu(μ-I)I and $LCu(\mu I)_2CuL$ are given in Fig. 3. It is assumed that Cu–Cu bond binding orbitals are mainly of d-character, and antibonding ones are of sp-character.

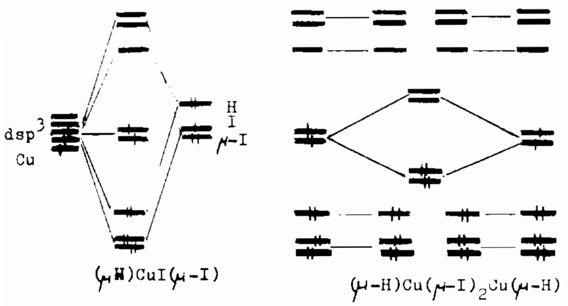

Fig. 3. Qualitative MO scheme for the $Cu_2I_2L_2$ moiety.

The IR spectroscopy analysis and geometry considerations suggest that the Ta and Cu atoms are bound by ordinary hydrogen bridges involving H_B atoms and acceptor–axial orbitals of Cu atoms (it is assumed that the geometry of the Cp_2TaH moiety by complex formation as well as of complexes $Cp_2TaH_3 \cdot ZnCl_2 \cdot THF$ [12] and **III** does not change). The H_A central atoms are not involved in the Cu atom bond formation because the latter lack relevant acceptor orbitals. This conclusion is supported by the presence of vibrations in the IR spectra of **I**, associated with the terminal bonds Ta–H (1740 cm^{-1}).

In the $[Cp_2ReH \cdot CuI]_2$ complex (**VI**) the H atom coordinates were not determined and an absorption band of ν(Re–H) terminal bond vibrations was not detected [4], although this bond is reliably stabilized in solution according to PMR spectra [19]. The absence of the Re–H terminal bond absorption in the IR spectra may be assigned to both a low signal intensity which is not very high even for pure Cp_2ReH and the Re–H–Cu bridge bond formation. However, since the H atom in Cp_2ReH is located on a symmetry axis of Cp_2Re – *z* wedge sandwich [20] – then the geometry of $[Cp_2ReH \cdot CuI]_2$ [4] and the very short Re–Cu distance (2.60 Å) suggest that the Re–Cu atoms binding occurs via interaction of d-electron lone pairs located on the b_2 orbital of the Cp_2Re moiety with the axial–acceptor orbital of the copper atom. Though the Cu–H distance in this complex is not large (1.7–2.2 Å depending on the Re–H bond deviation from the *z* axis), it may be assumed that the hydride atom contribution into the bond formation between Re and Cu atoms will be negligible.

As noted above short Cu–Cu contacts in complexes **I** and **VI** (2.60 and 2.55 Å [4]) causing rhombus $Cu(\mu\text{-}I)_2Cu$ bending along the I....I axis, from our viewpoint, can be assigned to the direct bond between copper(I) atoms. Since the two MO binding orbitals locate four electrons (Fig. 3), the Cu–Cu bond will be of the second order in this case.

In complex **III** the formation of the second (TaH_BCu) bridge bond is obviously caused by the interaction of the H atom 1s-orbital with the low antibonding ψ^*-orbital of the Cu–Cu bond (Fig. 3). However, only one of the two ψ^*-orbitals is occupied because of the symmetry in molecule **III**. Here, the copper–copper bond order should decrease to 1, which is well in accordance with a markedly increasing Cu–Cu distance in this complex (2.91 Å), the value of which is intermediate between that calculated for complex **I** (2.60 Å) and a disconnective contact in $[Cp_2MoH_2 \cdot CuI]_2$ (3.33 Å) [3].

The qualitative MO scheme for the $LCu(\mu_2\text{-}I)_2\text{-}CuL$ moiety means that direct bond formation between metals atoms becomes practically possible with the ratio L:Cu = 1:1. However, the realization of this condition solely is not sufficient for producing complexes with Cu–Cu bonds. Thus, coordination of ordinary bielectron n-bases would everytime yield complexes of CuI·L composition with the Cu atom in a tetrahedron environment (e.g. $CuI \cdot CH_3CN$).

Even copper(I) iodide complex formation with such a sterically hindered ligand such as $P[N(CH_3)_2]_3$ does not yield a complex with a Cu–Cu bond. According to the X-ray data this complex is a tetramer of composition $\{CuI \cdot P[N(CH_3)_2]_3\}_4$ (Fig. 4). Its Cu and I atoms are situated in corners of a distorted cube and are bound not by a direct Cu–Cu bond but by that of a μ_3-type. Coordination polyhedrons of copper atoms are distorted tetrahedrons with angles varying in the range 98–104° (Table 7). The Cu–Cu distances are apparently disconnective (3.28–3.46 Å). Thus, the tetrahedron environment of the phosphorus atom in molecule $P(NMe_2)_3$ does not necessarily create steric hindrances and there occurs an additional coordination of the iodide atom with the formation of an ordinary cubane structure typical for analogous compounds.

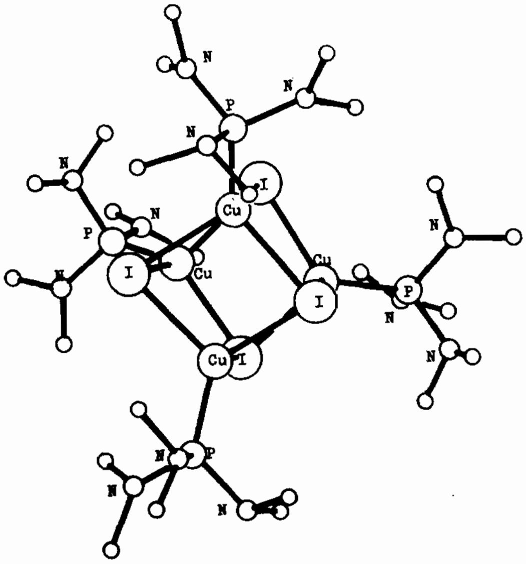

Fig. 4. The structure of the complex $\{Cu(\mu_3\text{-}I) \cdot P[N(CH_3)_2]_4\}$.

Thus, the Cu–Cu bond formation depends both on the L:Cu ratio and on a successful combination of space groups in the donor molecule preventing an intramolecular coordination of additional ligands (iodide atoms). These factors proved to be most effectively combined in copper-iodide-with-metallocene-hydrides complexes as well as with the molecules 2,2,6,6-tetramethylpiperidine [21] and 2,6-dimethylpyridine [22]. According to the X-ray analysis the latter compounds are dimers of $LCu(\mu_2\text{-}I)_2CuL$ composition. Although the $Cu(\mu_2\text{-}I)Cu$ rhombus bending along the I....I axis is not observed therein, heavy distorted valency angles and short Cu–Cu distances (2.53 and 2.59 Å respectively) are evidence in favour of a direct bond formation according to the scheme in Fig. 3.

An increased L:Cu ratio to 2:1 and more should lead to the occupation of the antibonding with respect to the Cu–Cu bond orbital and, consequently, to its rupture. Actually, in complexes with general formular $LLCu(\mu_2\text{-}I)_2CuLL$, the Cu–Cu contacts are disconnective, e.g. for L = quinoline at L:Cu = 2:1 this distance is 3.36 Å (see ref. 23 and refs. therein), whereas at L:Cu = 1:1 short Cu–Cu contacts (2.55 and 2.58 Å) [23] are realized though in a more complicated structure.

References

1 F. G. Mann, D. Purdie and A. F. Wells, *J. Chem. Soc.*, (1936) 1503.

2 J. P. Jasinski, N. R. Rath and E. M. Holt, *Inorg. Chim. Acta, 97* (1985) 91.

3 V. K. Bel'sky, E. B. Fomicheva, A. V. Aripovsky and B. M. Bulychev, *Dokl. AN SSSR, 258* (1981) 1137.

4 V. K. Bel'sky, V. M. Ishchenko, B. M. Bulychev and G. L. Soloveichik, *Polyhedron, 3* (1984) 749.

5 E. B. Lobkovsky, A. V. Aripovsky, V. K. Bel'sky and B. M. Bulychev, *Koord. Khim., 8* (1982) 104.

6 M. J. Bunker, A. Decian, M. L. H. Green, J. J. Moreau and N. Siganporia, *J. Chem. Soc., Dalton Trans.*, (1980) 2155.

7 R. Riemschneider and R. Nehrin, *Monatsch. Chem., 90* (1959) 569.

8 B. K. Vaidya, *Nature (London), 123* (1929) 414.

9 V. G. Andrianov, B. P. Biryukov and Yu. T. Struchkov, *Zh. Strukt. Khim., 10* (1969) 1123.

10 S. A. Semiletov, *Kristallografiya, 21* (1976) 752.

11 R. D. Wilson, T. F. Koetzle, D. W. Hart, A. U. Kvich, D. L. Tipton and R. Bau, *J. Am. Chem. Soc., 99* (1972) 1775.

12 T. M. Arkhireeva, B. M. Bulychev, T. A. Sokolova, G. L. Soloveichik, V. K. Bel'sky and G. N. Boiko, *Inorg. Chim. Acta, 141* (1988) 221.

13 Yu. K. Gun'ko, A. I. Sizov, B. M. Bulychev, V. K. Bel'sky and G. L. Soloveichik, *Metalloorg. Khim., 2* (1989) 1121.

14 R. A. Howie, G. P. McQuillan and D. W. Thompson, *J. Organomet. Chem., 268* (1984) 149.

15 L. F. Rhodes, J. C. Huffman and K. G. Caulton, *J. Am. Chem. Soc., 105* (1983) 5137.

16 A. Camus, N. Marsich, G. Nardin and L. Randaccio, *Inorg. Chim. Acta, 23* (1977) 131.
17 P. K. Mehrotra and K. Hoffmann, *Inorg. Chem., 17* (1978) 2187.
18 S. G. Gagarin and Yu. A. Teterin, *Zh. Neorg. Khim., 29* (1984) 1915.
19 V. M. Ishchenko, B. M. Bulychev and G. L. Soloveichik, *Koord. Khim., 9* (1983) 622.
20 I. W. Lauher and R. Hoffmann, *J. Am. Chem. Soc., 98* (1976) 1729.
21 P. C. Healy, C. Pakawatchai, C. L. Raston, B. W. Skelton and A. H. White, *J. Chem. Soc., Dalton Trans.,* (1983) 1905.
22 J. A. Campbell, *Aust. J. Chem., 30* (1977) 1937.
23 N. P. Rath, E. M. Holt and K. Tanimura, *J. Chem. Soc., Dalton Trans.,* (1986) 2303.